Heliyon 10 (2024) e35603

Contents lists available at ScienceDirect

Heliyon

journal homepage: www.cell.com/heliyon

Research article

The novel HSP90 monoclonal antibody 9B8 ameliorates articular cartilage degeneration by inhibiting glycolysis via the HIF-1 signaling pathway

Shunan Yu [a,1], Xiong Shu [a,1], Xinyu Wang [a], Yueyang Sheng [a], Shan Li [a], Ying Wang [a], Yanzhuo Zhang [a], Jiangfeng Tao [a], Xu Jiang [b,*], Chengai Wu [a,**]

[a] *Department of Molecular Orthopedics, Beijing Research Institute of Traumatology and Orthopedics, National Center for Orthopaedics, Beijing Jishuitan Hospital, Beijing, 100035, PR China*

[b] *Department of Orthopaedics, Beijing Jishuitan Hospital, Capital Medical University, Beijing Research Institute of Traumatology and Orthopaedics, Beijing, 100035, PR China*

ARTICLE INFO

Keywords:
Osteoarthritis
9B8
HSP90
Cartilage
Chondrocytes
HIF-1 signaling

ABSTRACT

Osteoarthritis (OA) is a prevalent chronic degenerative disease that affects the bones and joints, particularly in middle-aged and elderly individuals. It is characterized by progressive joint pain, swelling, stiffness, and deformity. Notably, treatment with a heat shock protein 90 (HSP90) inhibitor has significantly curtailed cartilage destruction in a rat model of OA. Although the monoclonal antibody 9B8 against HSP90 is recognized for its anti-tumor properties, its potential therapeutic impact on OA remains uncertain. This study investigated the effects of 9B8 on OA and its associated signaling pathways in interleukin-1β (IL-1β)−stimulated human chondrocytes and a rat anterior cruciate ligament transection (ACLT) model. A specific concentration of 9B8 preserved cell viability against IL-1β−induced reduction. In vitro, 9B8 significantly reduced the expression of extracellular matrix-degrading enzyme such as disintegrin and metallopeptidase-4 (ADAMTS4) of thrombospondin motifs, matrix metalloproteinase-13 (MMP-13), as well as cellular inflammatory factors such as tumor necrosis factor-α (TNF-α) and interleukin-6 (IL-6), which were upregulated by IL-1β.

In vivo, 9B8 effectively protected the articular cartilage and subchondral bone of the rat tibial plateau from ACLT-induced damage. Additionally, gene microarray analysis revealed that IL-1β substantially increased the expression of SLC2A1, PFKP, and ENO2 within the HIF-1 signaling pathway, whereas 9B8 suppressed the expression of these genes. Thus, 9B8 effectively mitigates ACLT-induced osteoarthritis in rats by modulating the HIF-1 signaling pathway, thereby inhibiting overexpression involved in glycolysis.

These results collectively indicate that 9B8 is a promising novel drug for the prevention and treatment of OA.

* Corresponding author. Department of Orthopaedics, National Center for Orthopaedics, Beijing Jishuitan Hospital, Capital Medical University, Beijing, 100035, PR China.

** Corresponding author. Chengai Wu, Department of Molecular Orthopedics, Beijing Research Institute of Traumatology and Orthopedics, National Center for orthopaedics, Beijing Jishuitan Hospital, Capital Medical University, Beijing, 100035, PR China.

E-mail addresses: xujiang@vip.163.com (X. Jiang), wuchengai@jst-hosp.com.cn (C. Wu).

[1] These authors contributed equally to this work.

https://doi.org/10.1016/j.heliyon.2024.e35603
Received 11 April 2024; Received in revised form 4 July 2024; Accepted 31 July 2024
Available online 8 August 2024

1. Introduction

Osteoarthritis (OA) is a chronic degenerative disease that affects bones and joints, predominantly observed in the middle-aged and elderly populations. Patients experience progressive symptoms such as joint pain, swelling, deformity, and stiffness that significantly impair daily activities [1–3]. The pathogenesis of OA remains poorly understood, necessitating urgent research into the primary molecular mechanisms driving its onset and progression. Treatment strategies vary with the disease stage, ranging from visco-supplementation injections or physiotherapy to manage pain and preserve joint mobility in early stage of OA [2,4–6], to total joint replacement surgery in advanced stages [6–8]. Despite these interventions, there is a notable absence of disease-modifying drugs or agents that could enhance joint homeostasis in OA [6,9]. Consequently, extensive research is essential to explore potential therapeutic drugs that might modify the degenerated joint phenotype in OA.

Articular cartilage, an avascular tissue, relies on oxygen diffusion from synovial fluid and subchondral bone, leading to sustain hypoxia throughout its lifespan [10]. Studies have demonstrated oxygen gradients in cartilage, with approximately 6 % oxygen at the articular surface and only 1 % at deeper joint layers [11]. Current research suggests that adaptation to this avascular environment is facilitated by hypoxic-inducing factors HIF-1 and HIF-2. Chondrocytes respond to hypoxic conditions by activating signaling pathways that enhance oxygen delivery and maintain cellular adaptation to preserve oxygen homeostasis. The critical role of these hypoxia signaling pathways in chondrobiology and related diseases is increasingly recognized [12–14]. The HIF family of proteins includes alpha and beta subgroups that function through heterodimers formation [15–17]. HIF-1α is expressed in both normal and OA afflicted chondrocytes [12]. The expression of HIF-1 and its target genes, Glut-1 and PGK-1, in OA cartilage correlates with degeneration of articular cartilage [18,19].

Based on our prior research [20,21], we developed a monoclonal antibody (9B8) targeting HSP90 by immunizing BLAB/c mice with T3A-A3 cells. Heat shock proteins (HSPs) are highly conserved molecular chaperones essential for various cellular functions, including protein folding, assembly, and degradation [22]. Bioinformatic analysis revealed significant changes in the gene expression of the HSP90 family in the synovial membranes of female osteoarthritis patients [23]. HSP90 inhibition has been shown to modulate matrix metalloproteinase (MMP) production [24–26]. Treatment with an HSP90 inhibitor markedly increased glycosaminoglycan levels and reduced cartilage degradation in a rat model of biomechanically induced OA [27]. Typically, the basal activity of HSP70/HSP90 is sufficient for the processing of newly synthesized proteins in cells. However, inhibiting the upregulation of HSP70/HSP90 may interfere with the formation of properly folded and active HIF-1α, leading to the management of misfolded HIF-1α via quality control systems [28–30].

Here, we employed a novel HSP90 antibody to treat OA induced by ACLT surgery in rats, finding significant improvements in cartilage degradation and subchondral bone remodeling. Further investigation elucidated the mechanism underlying this phenomenon, suggesting that the new HSP90 antibody holds potential as a novel treatment for osteoarthritis.

2. Materials and methods

2.1. Reagents and antibodies

TB Green® Premix Ex Taq™ (TaKaRa, Japan), TaKaRa MiniBEST Universal RNA Extraction Kit (TaKaRa, Japan), GLUT1 Polyclonal Antibody (Proteintech), PFKP Polyclonal Antibody (Proteintech), NSE/ENO2-Specific Polyclonal Antibody (Proteintech), PageRuler Prestained Protein Ladder (Thermo Scientific,26616), SuperSignal™ West Pico PLUS Chemiluminescent Substrate (Thermo Scientific, 34580), NuPAGE® Novex 4–12 % Bis-Tris Gel, 1.0 mm, 15 Well (Thermo, NP0323BOX), NuPAGE™ MES SDS Running Buffer (Thermo, NP0060).

2.2. Cell culture and treatments

Human primary chondrocytes were sourced from the Beijing Beina Chuanglian Institute of Biotechnology and cultured in an incubator at 37 °C with 5 % CO_2. These cells were maintained in essential media (DMEM/F12, Hyclone, Logan, UT, USA) supplemented with 10 % fetal bovine serum, 100 U/mL penicillin, and 100 μg/mL streptomycin. Upon reaching 80%–90 % confluence, the cells were trypsinized using trypsin (Gibgo). For our in vitro experiment, the assays replicated a minimum of three times [9].

2.3. Construction a of monoclonal antibodies library

Monoclonal antibody libraries were constructed following the standard protocol outlined previously [20]. T3A-A3 cells, harvested during the logarithmic growth phase, were washed twice with phosphate-buffered saline (PBS). A portion of these cells was suspended in PBS at a concentration of 1×10^7/ml, and 0.5 ml was administered intraperitoneally to six BALB/C mice (BFK Bioscience, Beijing, China). The remaining cells were treated with 4 % paraformaldehyde for 30 min, followed by two PBS washes. These cells were then suspended at 1×10^7/ml in PBS and 0.5 ml was injected subcutaneously into the same mice. Two weeks later, identical subcutaneous injections of fixed cells were administered for booster immunization on a weekly basis. After eight boosts, the serum antibody concentration in the mice was assessed using ELISA.

Spleen cells from the mouse with the highest serum titer were fused with SP2/0 cells. The SP2/0 cells were cultured in 2.5 % methylcellulose (Sigma, St. Louis, MO, USA) supplemented HAT medium under a 5 % CO_2 atmosphere at 37 °C. After eight to ten days

of culturing, a monoclonal library consisting 2976 clones was prepared. The hybridoma cells were maintained in complete DMEM growth medium (Invitrogen, Carlsbad, CA, USA). The hybridoma supernatant was collected, and antibody production and purification were conducted following standard protocols. The isotype of the antibody used was determined using a commercial isotyping kit (Southern Biotech, Birmingham, AL, USA).

2.4. Purification and Identification of antigen recognized by monoclonal antibody 9B8

To purify the antigen recognized by monoclonal antibody 9B8 from SPCA-1sphere cells, G agarose (GE, Boston, USA) was employed alongside long-range SDS-PAGE. Initially, SPCA-1 sphere cells were lysed with 200 μL of RIPA buffer (Beyotime Biotechnology, Beijing, China), which included a protease inhibitor cocktail (Roche, Basel, Switzerland). The cell lysates were centrifuged at 12,000 rpm to separate the protein supernatant, which was then mixed with 20 μL of agarose G and centrifuged at 3000 rpm for 5 min to eliminate non-specifically bound proteins. Subsequently, the protein supernatant was incubated with 20 μL of G agarose pre-conjugated with a 9B8 antibody (10 μL) overnight at 4 °C. Lastly, the mixture was centrifuged to discard the supernatant.

Proteins were eluted with PBS and resolved via 10 % SDS-PAGE. The results were visualized using Coomassie Brilliant Blue staining and Western blotting. The putative HSP90 band was excised from the SDS-PAGE gel and analyzed using LC-MALDI-TOF/TOF as described in Refs. [20,21]. The fragment sequences were subsequently searched and analyzed using the MASCOT database (http://www.matrixscience.com).

2.5. Immunoprecipitation

To further identify the antigen, immunoprecipitations were conducted. G agarose was pre-incubated with 10 μg of a commercial anti-HSP90 antibody (Abcam, Cambridge, UK), the purified 9B8 mAb, or their respective negative controls, which included normal murine IgG and rabbit IgG. Cells were subsequently lysed using 200 μL of RIPA buffer containing a protease inhibitor cocktail. Total cell extracts were incubated with G agarose, after which the proteins were collected.

The target protein was immunoprecipitated by incubating the supernatant with agarose-conjugated antibodies overnight at 4 °C. The samples were subsequently washed three times with PBS. Immunoprecipitation efficiency was verified by Western blotting using mAb 9B8 or a commercial anti-HSP90 antibody [20,21].

2.6. Cell viability assay

Cell viability was assessed using the Cell Counting Kit-8 (CCK-8) from Invitrogen. Primary human chondrocytes were cultured in 96-well plates at 5000 cells per well. Twelve hours post-seeding, IL-1β (10 ng/ml, Sigma) was introduced concurrently with varying concentrations of 9B8 (0, 25, 50, 100, 200 μg/ml). After incubation periods of 12, 24, and 48 h, the medium was replaced with a 10 % CCK-8 solution and incubated for an additional 2 h at 37 °C darkness. Absorbance was measured at 450 nm using automatic microplate reader. Cell viability in the control group was set at 100 % [9].

2.7. Real-time quantitative polymerase chain reaction (RT-qPCR)

The expression of cartilage markers MMP13, ADAMTS4, COL2A1, ACAN, TNF-α, and IL-6 was analyzed using quantitative

Table 1
Sequences of primers used in qRT-PCR.

Genes		Sequences
ENO2	Forward	CCTCATCAGCTCAGGTCTCTC
	Reverse	ATTGGCCCCAAACTTGGAT
SLC2A1	Forward	GAACTCTTCAGCCAGGGTCC
	Reverse	ACCACACAGTTGCTCCACAT
PFKP	Forward	GACTGGGTGTTCCTTCCAGA
	Reverse	CGTGACGACAAGCTCTTTGA
MMP13	Forward	CCCCTTCCCTATGGTGAT
	Reverse	AAGCCAAAGAAAGACTGC
ADAMTS4	Forward	ACCCAAGCATCCGCAATC
	Reverse	CAGGTCCTGACGGGTAAAC
COL2A1	Forward	GAAGGATGGCTGCACGAAAC
	Reverse	CGGGAGGTCTTCTGTGATCG
ACAN	Forward	CCAAACCAACCCGACAAT
	Reverse	GGGAGCTGATCTCATAGCG
TNF α	Forward	CCTCTCTCTAATCAGCCCTCTG
	Reverse	GAGGACCTGGGAGTAGATGAG
IL-6	Forward	ACTCACCTCTTCAGAACGAATTG
	Reverse	CCATCTTTGGAAGGTTCAGGTTG
GAPDH	Forward	ACAGTTGCCATGTAGACC
	Reverse	TTTTTGGTTGAGCACAGG

polymerase chain reaction (qPCR). Total RNA was extracted and purified employing the TaKaRa MiniBEST Universal RNA Extraction Kit (Takara, Japan) according to the manufacturer's protocol. RNA concentrations were quantified with a NanoDrop One spectrophotometer, and cDNA was synthesized using the PrimeScript II 1st Strand cDNA Synthesis Kit (Takara, Japan). Quantitative RT-PCR was conducted on the Applied Biosystems 7500 Fast Real-Time PCR System (Bio-Rad), utilizing a Bio-Rad PrimeScript RT reagent Kit with gDNA Eraser (Perfect Real Time) [9]. The primers applied in this study are detailed in Table 1. Gene expression levels were evaluated using the ΔΔCt method and normalized to the expression of GAPDH [9].

2.8. Western blotting analysis

Primary human chondrocytes were seeded in 6-well plates at a density of 2×10^5 cells/well. Twelve hours later, varying concentrations of 9B8 (0, 50, 100, 200 μg/ml) were administered alongside IL-1β (10 ng/ml). After 24 h, samples were harvested using a total protein extraction kit from Thermo Fisher Scientific. The cell lysate was centrifuged at 20,000 rpm for 10 min at 4 °C to remove cellular debris, and protein concentrations were measured using the Bradford method. Following electrophoresis, 15 μg of protein per well were transferred onto polyvinylidene fluoride membranes (Invitrogen). The membranes were blocked with 5 % non-fat milk in Tris-Buffered Saline and Tween 20 (TBST) for 60 min, then incubated overnight at 4 °C with primary antibodies diluted 1:1000. After six TBST washes of 5 min each, the membranes were incubated with appropriate mouse or rabbit IgG secondary antibodies at room temperature for 2 h. Immunoreactivity was detected using SuperSignal™ West Pico PLUS Chemiluminescent Substrate (Thermo). Relative protein expression levels in each group were quantified using Image J software [9].

2.9. Animal model and treatment

Male Sprague-Dawley (SD) rats, weighting between 180 g and 200 g, were procured from Beijing Vitonlihua Experimental Animal Technology Company with approval from the Experimental Ethics Committee at Beijing Jishuitan Hospital. The rats were housed under controlled conditions: single cage housing, unrestricted cage movement, temperatures of 18–23 °C, relative humidity of 50 %–60 %, a 12-h light/dark cycle, and ad libitum access to chow. The osteoarthritis model was established through anterior cruciate ligament transection (ACLT) surgery. Each rat received an intraperitoneal injection of 1 % sodium pentobarbital (30 mg/kg) for anesthesia [9]. Subsequent to effective anesthesia, the rat's right hind leg and lower abdomen were shaved. The surgery involved anterior and central incisions in the right posterior knee joint; exposing the knee after the skin was cut. A 2 cm curved incision was made along the medial side of the patella, from the proximal to the distal end. The patella was rotated posteriorly, exposing the knee. The anterior cruciate ligament was then severed using ophthalmic scissors, and the knee's stability was assessed via drawer testing. If instability was conformed, indicating a complete tear, the knee cavity was washed with saline, and the incision was sutured using 4-0 sutures. Postoperative recover was typically observed for about 40 min before the rats resumed normal activities, including eating and drinking [9].

For the study, 48 rats were randomly allocated into six groups: normal (n = 8), sham (n = 8), ACLT (n = 8), low dose 9B8 (0.125 mg/kg), medium dose 9B8 (0.5 mg/kg) and high dose 9B8 (2 mg/kg). Both ACLT and varying doses of 9B8 were administered to designated groups, except the sham group, which underwent a sham operation. Five weeks post-surgery, the respective doses of 9B8 were administered weekly via intraperitoneal injection. Twelve weeks post-surgery, the rats were euthanized for analysis.

2.10. Micro-Computed tomography (Micro-CT)

The tissue samples were fixed in 4 % polyformaldehyde for 48 h and subsequently submerged in a saline solution for 24 h before microimaging of the subarticular cartilage and subchondral bone in the right hind knee of a rat. Computed tomography scans, totaling 21 μM and each 70 kV, were conducted using Bruker Sky Scan 1176. The following parameters were quantified using CTAN software (version 1.17.7.2): bone mineral density (BMD), bone volume fraction (BV/TV), structural model index (SMI), number of trabeculae (Tb.N), trabecular separation (Tb.sp), and trabecular pattern factor (Tb.Pf). Knee three-dimensional reconstruction was carried out using the CTVox software (version 3.3.0r1403) [9,31].

2.11. Histological staining

Tissue samples were fixed in 4 % polyformaldehyde for 48 h, rinsed with tap water for 12 h, and subsequently decalcified using 12.5 % EDTA over eight weeks. The decalcified samples underwent dehydration using a series of ethanol gradients. Following embedding in paraffin and sectioning, sagittal sections of 5 μm thickness were stained with hematoxylin–eosin (HE; Solarbio) and safranin O-fast green (Safranin O; Solarbio) [9,31].

2.12. RNA extraction and gene expression analysis

Primary human chondrocytes were seeded into 6-well plates at a density of 2×10^5 cells per well. The experimental groups included normal (HN), IL-1β (HI), IL-1β + IgG (Sigma, I2511) (HG), IL-1β + Low (9B8: 50 μg/ml) (HL), IL-1β + Medium (9B8: 100 μg/ml) (HM), IL-1β + High (9B8: 200 μg/ml) (HH), with three replicates per group. After 12 h of culture, 9B8 and IL-1β (10 ng/ml) were co-cultured at varying concentrations. RNA extraction was performed 24 h later using the TRIZol RNA purification kit (Invitrogen). The RNA microarray detection procedure involved: (1) Preparation and quality control of total RNA samples, where RNA

concentration and purity were assessed using a NanoDrop microspectrophotometer; the integrity of RNA and presence of DNA contamination were analyzed via agarose gel electrophoresis, and microRNA concentration was precisely quantified. (2) Library construction and quality assessment involved total RNA (with added PolyA control) being used for synthesis of cDNA's first and second strands, followed by in vitro purification, quantification, and dilution to 625 ng/μl. The synthesized second cycle singlet cDNA was then diluted to 31.2 μl with 5.5 μg of sscDNA in enzyme-free water for subsequent fragmentation and labeling. (3) Hybridization, washes, and scanning: Chip hybridization samples were added to the Clariom D Human chip and subjected to hybridization in a GeneChip Hybridization Oven 645 at set temperatures and rates; post-hybridization, chips were washed using the d GeneChip Fluidics Station 450 with stipulated protocols and scanned with the GeneChip 3000 7G scanner. CEL files, representing fluorescence signal, were generated and converted to probe signal values using GCOS software. (4) Data analysis involved GO Enrichment Analysis and Pathway Enrichment Analysis. The microarray experiment was carried out by Beijing Cnkingbio Biotechnology Corporation [9].

2.13. Statistical analysis

All data were presented as mean ± standard deviation. Two-way or one-way analysis of variance (ANOVA) was utilized to compare group means, supplemented by Fisher's LSD test for multiple comparisons. Data within the same group were analyzed using Student's

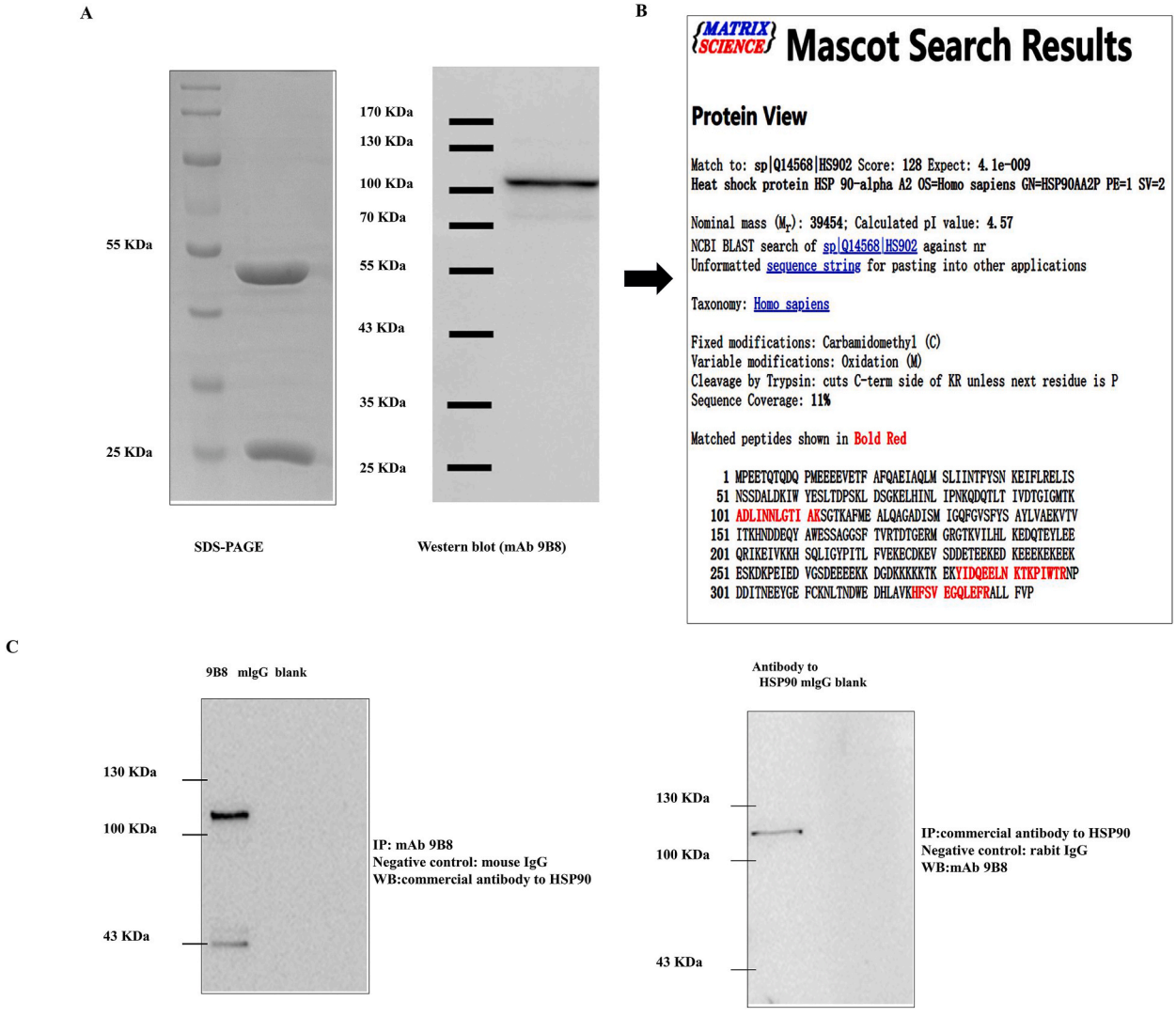

Fig. 1. Identification of the Targeted Antigen Recognized by mAb 9B8.
A. Purification of antigen recognized by mAb 9B8 from the cell lysate of SPCA-1 sphere cells. Protein were electrophoresed (right panel) and immunoblotted with mAb 9B8 (left panel). B. A protein band excised from SDS-PAGE was identified as HSP90α using mass spectrometry and n Mascot database analysis. C. Identification of mAb 9B8-binding antigen by Immunoprecipitation-Western blot. Immunoprecipitation using purified mAb 9B8 or a commercial antibody against HSP90α was followed by Western blotting for HSP90. Results confirmed the interaction between the HSP90α antigen and mAb 9B8 in a protein band.

t-test. Significance levels were established at × P < 0.05, **P < 0.01, ***P < 0.001.

3. Result

3.1. Identification of HSP90 as an antigen for mAb 9B8 antigen

In this study, we aimed to purify and identify the antigen targeted by mAb 9B8. To ascertain the specific antigens recognized by mAb 9B8, cell lysates from SPCA-1 sphere cells were subjected to purification using G agarose, followed by electrophoresis and immunoblotting with the 9B8 antibody. Coomassie brilliant blue staining revealed a protein band that was further verified via Western blot analysis (Fig. 1A). Subsequently, protein bands isolated from SDS-PAGE were analyzed using LC-MALDI-TOF/TOF mass spectrometry. To determine whether the antigen targeted by mAb 9B8 was human HSP90α, a Mascot database search was conducted (Fig. 1B). Further confirmation of HSP90α as the target antigen of mAb 9B8 was achieved through immunoprecipitations performed using either a commercial antibody against HSP90α or purified mAb 9B8. The protein band was shown via immunoprecipitation to interact with either mAb 9B8 or the commercial antibody against HSP90α (Fig. 1C). Collectively, these results strongly indicate that HSP90α is the target antigen for mAb 9B8.

3.2. The effect of 9B8 on chondrocyte viability

To investigate the impact of 9B8 on chondrocyte viability, chondrocytes were exposed to different concentrations of 9B8 for various durations (6, 12, 24, and 48 h) in a CCK-8 assay. The results indicate that within 24 h, 9B8 concentrations ranging from 0 to 400 μg/ml did not significantly affect the viability primary human chondrocytes (Fig. 2A). Furthermore, we examined the effect of 9B8 on IL-1β-induced changes in chondrocyte activity. At concentrations of 25, 50, 100, and 200 μg/ml, 9B8 partially restored the IL-1β-induced

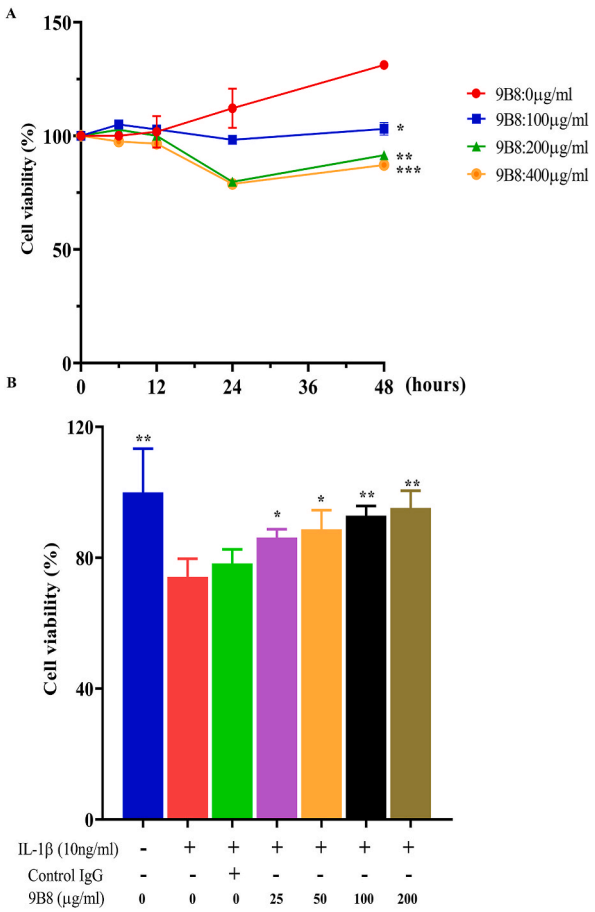

Fig. 2. 9B8 Alleviates the Decrease in Cell Viability Induced by Interleukin (IL)-1βA. Cell viability was assessed following stimulation with IL-1β (10 ng/ml) and varying concentrations of 9B8 (0, 25, 50, 100, 200 μg/ml) at different time points. B. Cell viability following IL-1β (10 ng/ml) stimulation after pre-treatment with various concentrations of 9B8 (0, 25, 50, 100, 200 μg/ml). All experiments were conducted at least three times, and the data are presented as mean ± standard deviation. *p < 0.05, **p < 0.01, ***p < 0.001 ****p < 0.0001 compared with the IL-1β−treated groups.

decline in chondrocyte function after 24 h (Fig. 2B).

3.3. The impact of 9B8 on Chondrocyte Metabolism and inflammatory factors

We subsequently investigated the impact of 9B8 on the expression of metabolism-related genes (COL2A1, ACAN, ADAMTS4 and MMP13) in chondrocytes. Fig. 3 demonstrated that IL-1β reduced the expression of COL2A1 and ACAN while increasing the expression of MMP13 and ADAMTS4 in chondrocytes. Treatment with 9B8 at concentrations of 50, 100, and 200 μg/ml mitigated these changes to varying extents (Fig. 3A and B). Additionally, we examined the effects of 9B8 on inflammatory factors. We found that 9B8 significantly inhibited the expression of TNF-α and IL-6, showing an anti-inflammatory effect comparable to that of dexamethasone (Fig. 3C). These findings collectively suggest that 9B8 can inhibit catabolism, enhance the accumulation of extracellular matrix collagen and proteoglycans, and reduced the levels of the inflammatory markers TNF-α and IL-6.

3.4. 9B8 Ameliorates ACLT-induced osteoarthritis in rats

To assess whether 9B8 can mitigate osteoarthritis in vivo, we employed a rat ACLT model to induce cartilage degeneration. The experimental groups and the sequence of procedures are delineated in Fig. 4A. At 12 weeks, the appearance of the knee joints revealed substantial cartilage degeneration and osteophyte formation in the ACLT group compared to the normal group on the tibial plateau (Supplementary Fig. 1). Increased doses of 9B8 were associated with reduced osteophyte formation in the tibial plateau (Supplementary Fig. 1). Having confirmed 9B8's protective effects on subchondral bone, we conducted HE and Safranin O staining to examine the impact of 9B8 on the articular cartilage of the medial tibial plateau in rats. As depicted in Fig. 4B, ACLT induced significant chondrocyte loss and fibrillation. However, intraperitoneal injections of 9B8 (medium and high dose) significantly reduced the destruction of the articular cartilage compared with the ACLT group. The OARSI score further confirmed that 9B8 ameliorated ACLT-induced cartilage damage (Fig. 4C).

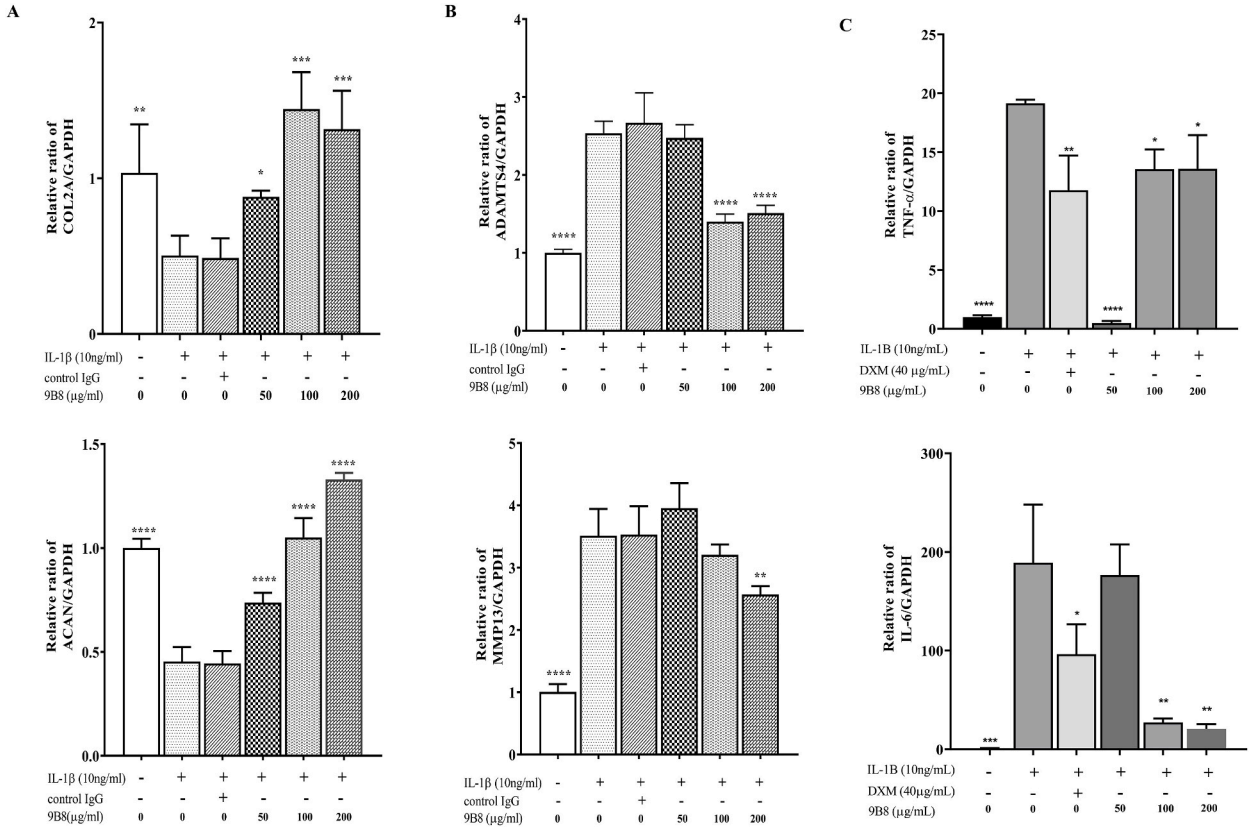

Fig. 3. 9B8 Inhibited IL-1β-Induced Enhancement of Chondrocyte Metabolism and Inflammatory Factors.
A, B. The relative mRNA expression levels of COL2A1, ACAN, MMP13, and ADAMTS4 were assessed in chondrocytes stimulated with IL-1β (10 ng/ml) and varying concentrations of 9B8 (0, 50, 100, 200 μg/ml) at 24 h using qRT-PCR. C. The relative mRNA expression levels of TNF-α and IL-6 were assessed in chondrocytes stimulated with IL-1β (0 or 10 ng/ml) and varying concentrations of 9B8 (50, 100, 200 μg/ml) or Dexamethasone at 24 h using qRT-PCR.All experiments were conducted at least three times, and data are presented as mean ± standard deviation. *$p < 0.05$, **$p < 0.01$, ***$p < 0.001$, and****$p < 0.0001$ compared with IL-1β−treated groups.

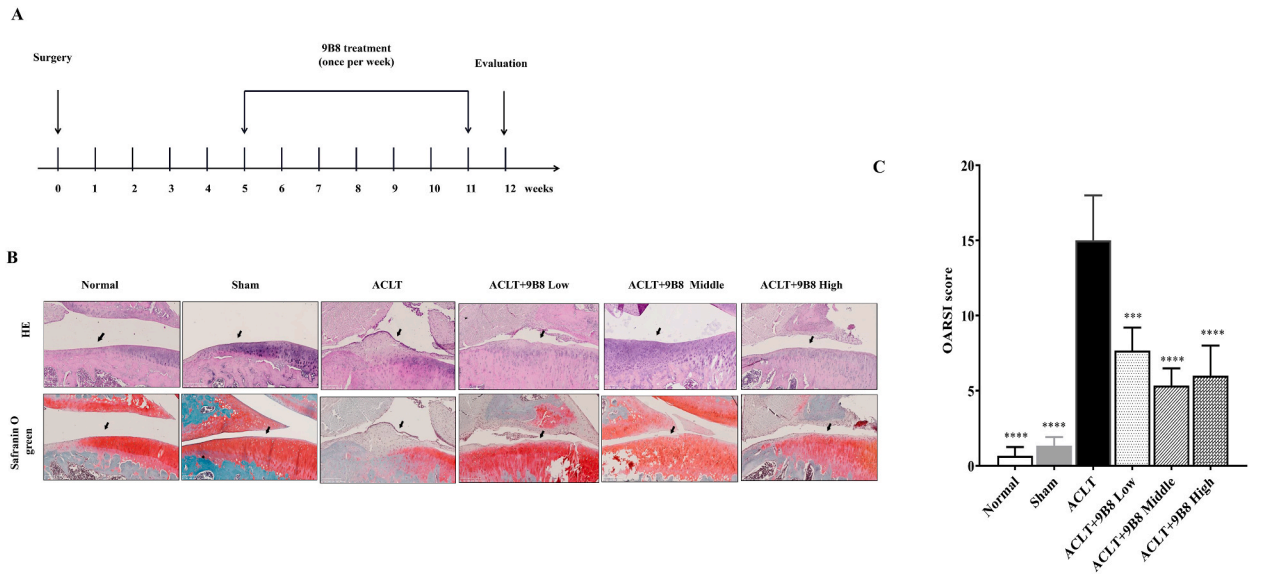

Fig. 4. 9B8 Inhibits ACLT-Induced Destruction of Knee Articular Cartilage.
A. Rat grouping and animal testing procedures. B. Representative HE staining and safranin O-fast green staining images of right knee joints in rats, 12 weeks post-surgery across all groups. C. Cartilage OARSI scores for different groups. All experiments were conducted at least three times, and data are presented as mean ± standard deviation. Statistically significant differences are indicated by × $p < 0.05$, **$p < 0.01$, ***$p < 0.001$, and ****$p < 0.0001$ compared with ACLT groups.

3.5. 9B8 Alleviates ACLT-Induced Subchondral Bone Destruction in rats

Qualitative and quantitative analyses of the knee joint were conducted using micro-CT. A three-dimensional reconstruction of the knee in 12-week postoperative rats is presented in Fig. 5A. The bone surface in the ACLT group was irregular, exhibiting significant

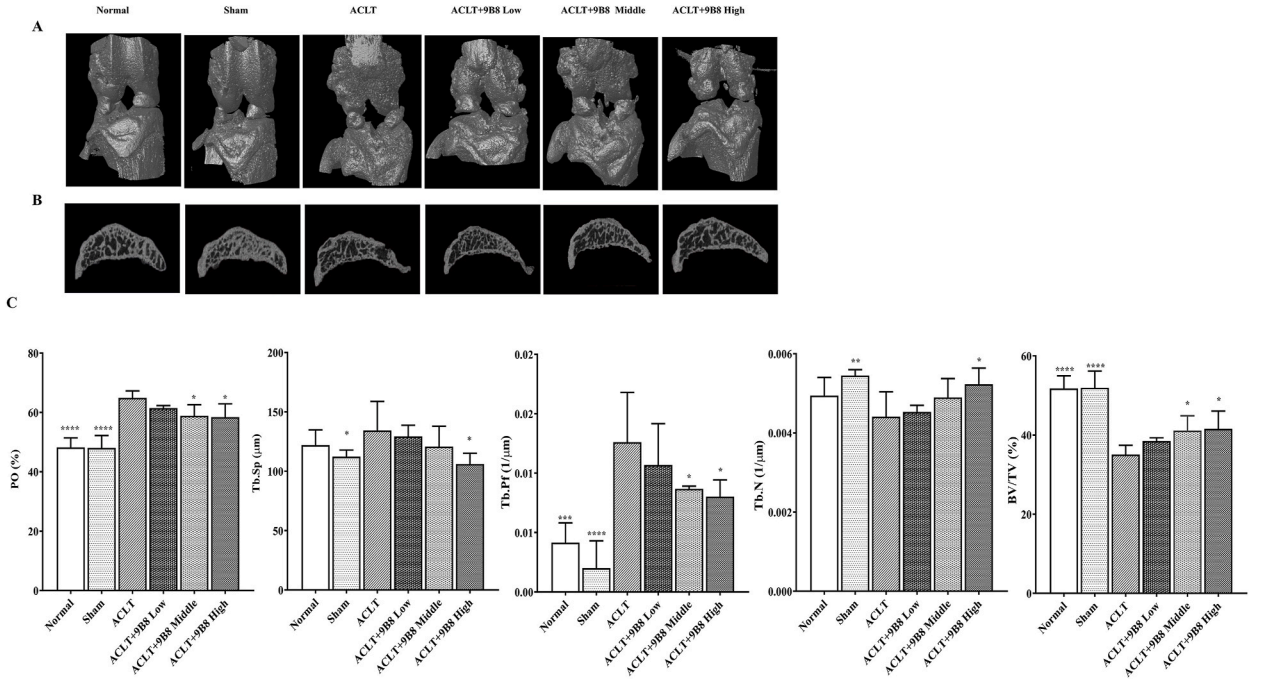

Fig. 5. 9B8 Inhibits ACLT-Induced Subchondral Bone Destruction in Rat Knee Joints.
A. 3D reconstruction of a rat's right knee using micro-CT, 12 weeks post-operation. B. Sagittal subcartilaginous images of the medial tibial plateau in rats from micro-CT scans. C. Quantitative analysis of micro-CT parameters of the medial subchondral bone of the right tibial plateau in rats. Data are presented as mean ± standard deviation. *$p < 0.05$, **$p < 0.01$, ***$p < 0.001$, and ****$p < 0.0001$ compared with ACLT groups.

osteophyte formation, in contrast to the normal group. Notably, the low-, medium-, and high-dose groups showed considerable improvements compared to the ACLT group. Micro-CT also detected alteration in the subarticular bone of the rat knee joints (Fig. 5B). Specifically, the sagittal plane in the ACLT group revealed irregular bone vesicles and numerous protrusions within the tibial plateau subchondral bone at 12 weeks. Conversely, the tibial tray subchondral bone in the treatment groups appeared relatively continuous compared to the normal group. Additionally, quantitative micro-CT analysis indicated that 9B8 counteracted the effects on BV/TV, PO, Tb.N, Tb.Sp, and Tb.Pf (Fig. 5C). Overall, intraperitoneal injections of 9B8 mitigated the ACLT-induced damage in the subchondral bone of the tibial plateau in rats.

3.6. 9B8 Ameliorates IL-1β-induced Chondrocyte Inflammation through the HIF1α signaling pathway

After confirming the protective effects of 9B8 on chondrocytes in vitro and articular cartilage in vivo, we aimed to determine the underlying mechanism of 9B8's protective action against OA. We examined the transcriptome of primary human chondrocytes treated with IL-1β, followed by 9B8 administration, using the Calriom D assay. As depicted in Fig. 6A, differentially expressed genes were selected to calculate correlations between various sample groups, clustering together to suggest similar biological functions within the same cluster. Subsequent analysis of changes in signaling pathways revealed that the HIF-1 signaling pathway was significantly up-regulated following IL-1β stimulation but suppressed post-9B8 treatment (Fig. 6B). Specifically, IL-β up-regulated twelve genes in the HIF-1 signaling pathway, while 9B8 treatment down-regulated ten genes Table 2. Notably, three genes-ENO2, SLC2A1, and PFKP-

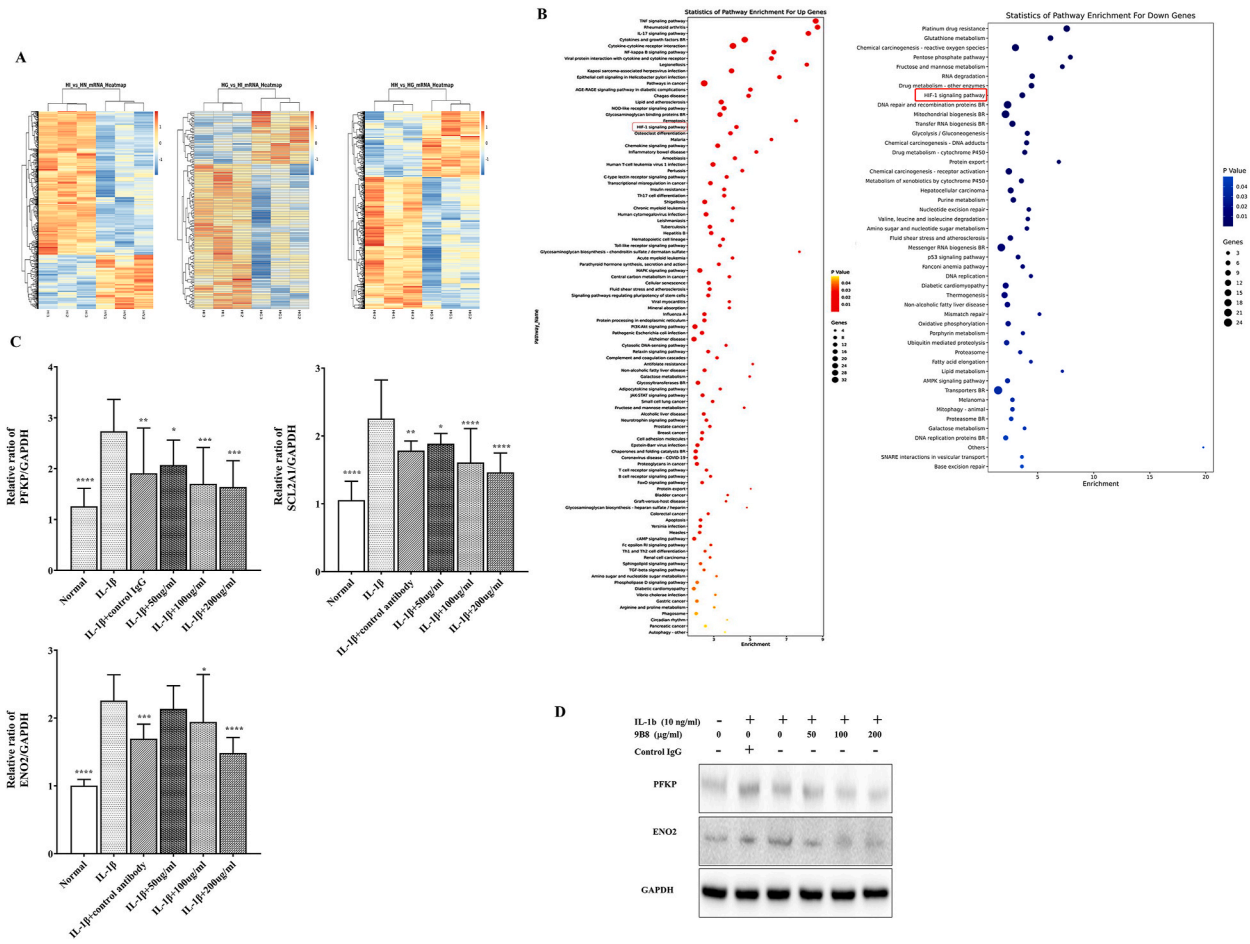

Fig. 6. 9B8 Inhibits IL-1β-induced Enhancement of Chondrocyte Inflammation via the HIF1 Signal Pathway.
A. Primary human chondrocytes were treated with varying concentrations of 9B8 (0, 50, 100, 200 μg/ml) and IL-1β (10 ng/ml). After 24 h of incubation, unsupervised hierarchical clustering analysis was performed to illustrate the differential mRNA expression using heat maps, where red indicates up-regulation and green indicates down-regulation. B. Alterations in the expression of signaling pathway between groups. C. Relative mRNA expression of PFKP, SLC2A1, and ENO2 in chondrocytes stimulated with IL-1β (10 ng/ml) and various concentrations of 9B8 (0, 50, 100, 200 μg/ml) at 24 h, measured by qRT-PCR. D. Protein levels of PFKP and ENO2 in chondrocytes treated with IL-1β (10 ng/ml) and different concentrations of 9B8 (0, 50, 100, 200 μg/ml) were analyzed using Western blot. All experiments were conducted at least three times. Data are presented as mean ± standard deviation. Significance levels are denoted as × $p < 0.05$, ** $p < 0.01$, *** $p < 0.001$, and **** $p < 0.0001$ compared with IL-1β treated groups.

were commonly regulated by both IL-1β and 9B8. RT-qPCR data demonstrated that the mRNA level of ENO2, SLC2A 1, and PFKP decreased relative to the positive control group as the concentration of 9B8 increased (Fig. 6C). Western blot results further confirmed that 9B8 elevated the protein levels of ENO2 and PFKP (Fig. 6D). Given that PFKP and ENO2 are involved in the glycolysis pathway, with PFKP being a key step, we conclude that the novel 9B8 antibody targeting HSP90 inhibits OA progression by impeding glycolysis via the HIF-1α signaling pathway (Fig. 7).

4. Discussion

Osteoarthritis (OA) is a chronic and degenerative disorder. Despite ongoing research into its pathogenesis and treatment, there is currently no effective means to halt OA progression due to challenges associated with cartilage regeneration post-injury [32]. Our study introduces a novel HSP90 antibody, 9B8, which inhibits OA both in vitro and in vivo. We demonstrated that 9B8 suppressed the IL-1-β-activated HIF1α signaling pathway in primary human chondrocytes, reducing catabolism and thereby increasing in the production of Type II collagen and proteoglycan. Furthermore, 9B8 effectively mitigated ACLT-induced lesions in the subchondral bone and articular cartilage of rat tibial platforms. In conclusion, our findings suggest that 9B8, through the inhibiting the HIF-1 signaling pathway, may regulate cellular glucose metabolism and offer a novel therapeutic strategy for osteoarthritis.

Inflammatory factors, including tumor necrosis factor alpha, interleukin-1, and extracellular matrix proteolytic enzymes such as matrix metalloproteinases and aggrecanase, play a crucial role in the onset and progression of arthritis. Studies indicate that drugs targeting these factors have demonstrated significant efficacy in clinical trials and in vitro experiments. However, these medications also present certain adverse reactions. Due to individual variability, patients respond differently to these drugs. Consequently, clinicians must consider the patient's specific condition, disease progression, drug tolerance, cost, and other relevant factors when selecting treatments. Overall, monoclonal antibodies have exhibited significant potential in managing osteoarthritis.

In our previous study, we identified the monoclonal antibody 9B8 and demonstrated its antitumor effect [20]. Building on this, we purified monoclonal antibody 9B8 and investigated its role as a targeted antigen in osteoarthritis. We also confirmed HSP90α as the target antigen of mAb 9B8 using the immunoprecipitation technique (Fig. 1C).

In this study, we demonstrated that 9B8 inhibited the IL-1β-induced decrease in chondrocyte activity and downregulated the expressions of ADAMTS4 and MMP13 in vitro (Fig. 3). Dexamethasone, an adrenocortical hormone drugs, can reduce inflammatory responses by inhibiting the production of inflammatory mediators and inflammatory cells. It is used to treat diseases such as arthritis. In our study, we found that 9B8 inhibited the production of inflammatory mediators comparably to dexamethasone (Fig. 3).

The pathogenesis of OA is a multifaceted process, with numerous studies indicating that subchondral bone degeneration precedes articular cartilage deterioration in OA [33]. In this study, we employed ACLT as a rat model for OA [9,34] aiming to mitigate joint degeneration through intraperitoneal injections of 9B8, administered five weeks post-surgery. We utilized micro-CT to examine and assess the subchondral bone in the knee joint and tibial plateau. The finding revealed that ACLT induced significant damage to the bone and trabecular structures of the subchondral bone. Compared to the ACLT group, the intraperitoneal injection of 9B8 mitigated the damage to subchondral bone and demonstrated dose-dependent effects on certain parameters (Fig. 5).

Hypoxia-inducible factor 1 (HIF-1) is a heterodimeric protein composed of two subunits: HIF-1α and HIF-1β. HIF-1 is instrumental in activating the transcription of numerous genes coding for proteins involved in various cellular processes, including angiogenesis, glucose metabolism, cell proliferation/survival, and invasion/metastasis. A mouse model with chondrocyte-specific HIF-1 knockout demonstrated extensive chondrocyte death across all cartilage [35]. In epiphyseal chondrocytes, HIF-1 is crucial for maintaining anaerobic glycolysis and facilitating the synthesis of the extracellular matrix [36]. Chondrocytes in osteoarthritis may depend on adaptations in HIF-1 to preserve ATP levels and continue matrix synthesis [19].

After verifying the antagonistic effects of compound 9B8 on OA in both in vitro and in vivo models, we investigated the potential mechanism of action using RNA microarray analysis. Several signaling pathways activated by IL-1β were subsequently downregulated following treatment with 9B8. Notably, the HIF-1 signaling pathway emerged as a probable candidate due to its recognized involvement in OA. RNA microarray data indicated that IL-1β induced the upregulation of 11 genes in the HIF-1 signaling pathway in

Table 2
Changes of mRNA expression in HIF-1 signaling pathway in chondrocyte.

Upgenes/ IL-1b-induced chondrocyte	Downgenes/ Treatment of IL-1b induced chondrocytes with 9B8/
IL6	EIF4EBP1
NFKB1	VEGFA
MAP2K1	PGK1
EGLN1	PDK1
TFRC	CDKN1A
SERPI	PFKL
NE1	ALDOC
ENO2	ENO2
SLC2A1	SLC2A1
PFKP	PFKP
HK2	
EDN1	
PFKFB3	

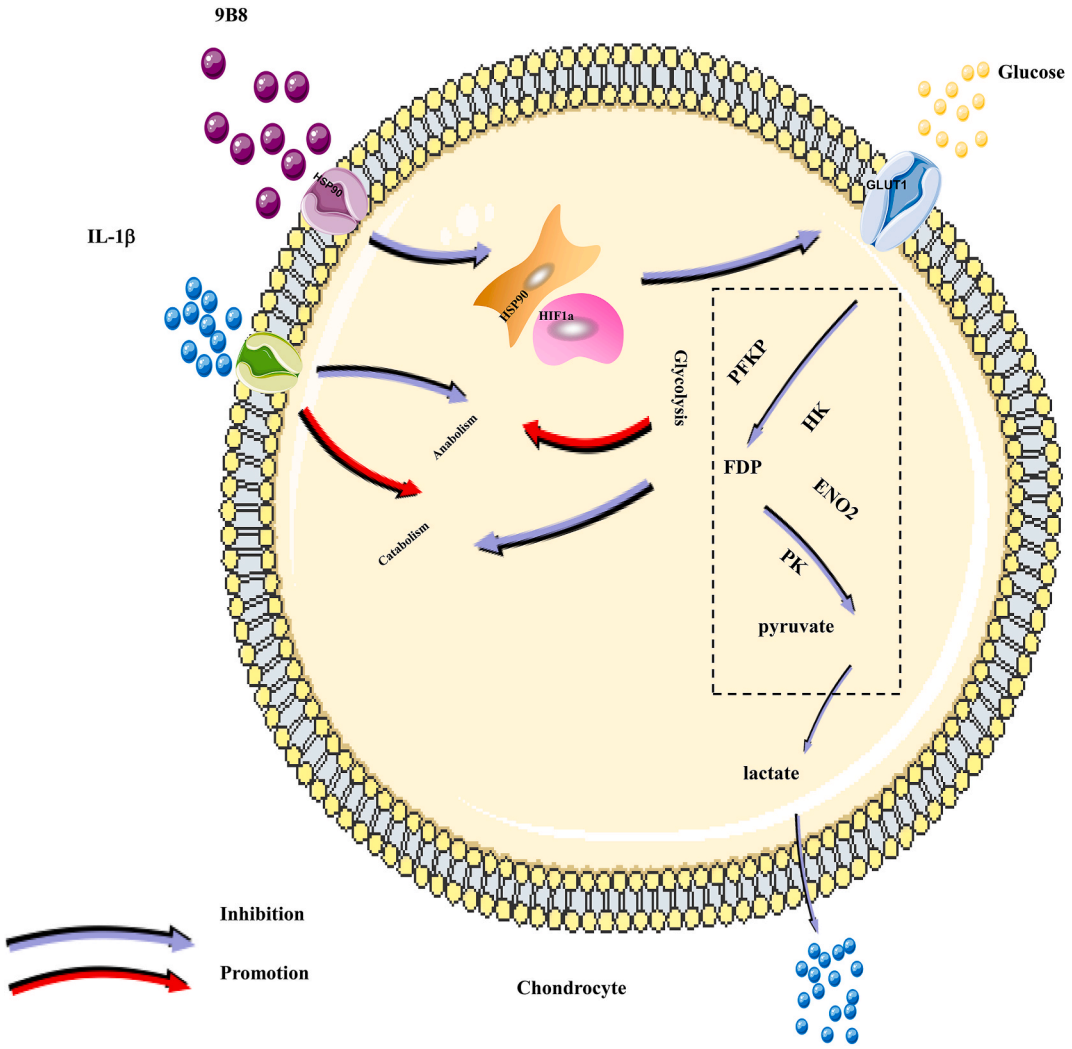

Fig. 7. Schematic Diagram of the potential protective effects of 9B8 on IL-1β-induced inflammatory injury in chondrocytes.

chondrocytes, whereas 9B8 treatment led to the downregulation of 9 genes, with ENO2, SLC2A 1, and PFKP being common to both conditions. SLC2A1 is known to modulate glucose transporters, enabling chondrocytes to adapt to varying extracellular glucose concentrations [37]. PFKP, which regulates glycolysis levels, has been linked to the proliferation of lung cancer cells.

During the development of OA, chondrocytes exhibit enhanced glycolytic activity and mitochondrial dysfunction [38,39]. Given the crucial role of glycolysis in OA, enzymes and processes involved in this pathway may contribute to its pathogenesis. Therefore, targeting glycolytic pathways to modulate OA metabolism could represent a significant advancement in treatment strategies for osteoarthritis. Although several natural products have recently shown the ability to regulate glycolysis, but their safety remains to be evaluated [40].

The purpose of this study was to determine whether the novel HSP90 antibody, 9B8, inhibits glycolysis overexpression in OA chondrocytes by suppressing the HIF-1a signaling pathway. The antibody 9B8 down-regulated the expression of PFKP and ENO2 in OA chondrocytes, both of which are components of the HIF-1a signaling pathway. Given that PFKP play a crucial role in glucose uptake and the regulation of glycolysis rates, it is proposed that 9B8 modulates glucose metabolism in OA chondrocytes through the regulation of the HIF-1a signaling pathway.

In conclusion, our study demonstrates for the first time the anti-catabolic effects of 9B8, a novel HSP90 monoclonal antibody, on chondrocytes. We found that 9B8 effectively mitigates ACLT-induced damage to articular cartilage and subchondral bone in rats. This effect might be mediated via the inhibition of HIF-1 signaling and subsequent glycolysis in chondrocytes. Collectively, our findings highlight the potential of 9B8 as a promising therapeutic agent for the effective treatment of OA.

This study has certain limitations. While we demonstrate the protective effects of 9B8 on chondrocytes and articular cartilage, the precise mechanisms by which it influences glycolysis have yet to be elucidated. The novel HSP90 9B8 antibody could potentially serve as a treatment for osteoarthritis in the future.

5. Conclusions

In conclusion, our study is the first to demonstrate the anti-catabolic effects of 9B8, a novel HSP90 monoclonal antibody, on chondrocytes. Additionally, 9B8 effectively mitigates ACLT-induced damage to articular cartilage and subchondral bone in rats. The mechanism underlying these effects may involve the inhibition of HIF-1mediated glycolysis in chondrocytes. Collectively, these findings suggest that 9B8 holds potential as a therapeutic agent for the effectively treating OA.

Ethics approval and consent to participate

All procedures of the animal experiments were approved by the Beijing Jishuitan Hospital Animal Care and Use Committee (Number: JST-202103-02), Beijing, China and performed in accordance with the institutional guidelines for care and use of animals.

Data availability statement

All data in the current study are available from Cheng-Ai Wu author upon reasonable request.

Consent for publication

Not applicable.

Availability of data and materials

All data in the current study is available from authors upon reasonable request.

Funding information

This study was supported by the National Natural Science Foundation of China (Grant No. 82202719), the Beijing Natural Science Foundation - Haidian Original Innovation Joint Fund (Grant No., L222089) and the Beijing Municipal Health Commission (Grant Nos., BJRITO-RDP-2024, XT-2024-05/06), Beijing.

CRediT authorship contribution statement

Shunan Yu: Writing – original draft, Investigation, Data curation, Conceptualization. **Xiong Shu:** Writing – original draft, Methodology, Investigation, Data curation, Conceptualization. **Xinyu Wang:** Methodology, Data curation, Conceptualization. **Yueyang Sheng:** Methodology, Data curation, Conceptualization. **Shan Li:** Methodology, Data curation, Conceptualization. **Ying Wang:** Project administration, Conceptualization. **Yanzhuo Zhang:** Methodology, Data curation. **Jianfeng Tao:** Methodology, Data curation. **Xu Jiang:** Writing – review & editing, Project administration, Funding acquisition. **Chengai Wu:** Writing – review & editing, Project administration, Funding acquisition.

Declaration of competing interest

We declare that we have no financial and personal relationships with other people or organizations that can inappropriately influence our work, there is no professional or other personal interest of any nature or kind in any product, service and/or company that could be construed as influencing the position presented in, or the review of, the manuscript entitled.

Acknowledgements

Not applicable.

Abbreviations

ACLT	anterior cruciate ligament transection
ACAN	aggrecan
ADAMTS4	a disintegrin and metalloproteinase with thrombospondin motifs 4
BMD	bone mineral density
BV/TV	bone volume fraction
Col2	collagen II
ECM	extracellular matrix
IL-1β	Interleukin-1β
MMP13	matrix metallopeptidase-13
OA	osteoarthritis

OARSI Osteoarthritis Research Society International
Tb. N: trabecular number
Tb. Pf trabecular bone pattern factor
Tb. Sp: trabecular separation
Micro-CT micro-computed tomography

Appendix A. Supplementary data

Supplementary data to this article can be found online at https://doi.org/10.1016/j.heliyon.2024.e35603.

References

[1] X. Wang, T. Liu, C. Qiu, S. Yu, Y. Zhang, Y. Sheng, C. Wu, Characterization and role exploration of ferroptosis-related genes in osteoarthritis, Front. Mol. Biosci. 10 (2023) 1066885, https://doi.org/10.3389/fmolb.2023.1066885.
[2] J.G. Quicke, P.G. Conaghan, N. Corp, G. Peat, Osteoarthritis year in review 2021: epidemiology & therapy, Osteoarthritis Cartilage 30 (2) (2022) 196–206, https://doi.org/10.1016/j.joca.2021.10.003.
[3] B. Abramoff, F.E. Caldera, Osteoarthritis: pathology, diagnosis, and treatment options, Med. Clin. 104 (2) (2020) 293–311, https://doi.org/10.1016/j.mcna.2019.10.007.
[4] N.K. Arden, T.A. Perry, R.R. Bannuru, O. Bruyère, C. Cooper, I.K. Haugen, M.C. Hochberg, T.E. McAlindon, A. Mobasheri, J.Y. Reginster, Non-surgical management of knee osteoarthritis: comparison of ESCEO and OARSI 2019 guidelines, Nat. Rev. Rheumatol. 17 (1) (2021) 59–66, https://doi.org/10.1038/s41584-020-00523-9.
[5] R.R. Bannuru, M.C. Osani, E.E. Vaysbrot, N.K. Arden, K. Bennell, S.M.A. Bierma-Zeinstra, V.B. Kraus, L.S. Lohmander, J.H. Abbott, M. Bhandari, F.J. Blanco, R. Espinosa, I.K. Haugen, J. Lin, L.A. Mandl, E. Moilanen, N. Nakamura, L. Snyder-Mackler, T. Trojian, M. Underwood, T.E. McAlindon, OARSI guidelines for the non-surgical management of knee, hip, and polyarticular osteoarthritis, Osteoarthritis Cartilage 27 (11) (2019) 1578–1589, https://doi.org/10.1016/j.joca.2019.06.011.
[6] O. McClurg, R. Tinson, L. Troeberg, Targeting cartilage degradation in osteoarthritis, Pharmaceuticals 14 (2) (2021) 126, https://doi.org/10.3390/ph14020126.
[7] M.C.M. van Doormaal, G.A. Meerhoff, T.P.M. Vliet Vlieland, W.F. Peter, A clinical practice guideline for physical therapy in patients with hip or knee osteoarthritis, Muscoskel. Care 18 (4) (2020) 575–595, https://doi.org/10.1002/msc.1492.
[8] D. Apostu, O. Lucaciu, A. Mester, D. Oltean-Dan, M. Baciut, G. Baciut, S. Bran, F. Onisor, A. Piciu, R.D. Pasca, A. Maxim, H. Benea, Systemic drugs with impact on osteoarthritis, Drug Metab. Rev. 51 (4) (2019) 498–523, https://doi.org/10.1080/03602532.2019.1687511.
[9] Z. Wu, Y. Wang, G. Yan, C. Wu, Eugenol protects chondrocytes and articular cartilage by downregulating the JAK3/STAT4 signaling pathway, J. Orthop. Res. 41 (4) (2023) 747–758, https://doi.org/10.1002/jor.25420.
[10] P.I. Milner, T.P. Fairfax, J.A. Browning, R.J. Wilkins, J.S. Gibson, The effect of O2 tension on pH homeostasis in equine articular chondrocytes, Arthritis Rheum. 54 (11) (2006) 3523–3532, https://doi.org/10.1002/art.22209.
[11] I.A. Silver, Measurement of pH and ionic composition of pericellular sites, Philos. Trans. R. Soc. Lond. B Biol. Sci. 271 (912) (1975) 261–272, https://doi.org/10.1098/rstb.1975.0050.
[12] I.B. Coimbra, S.A. Jimenez, D.F. Hawkins, S. Piera-Velazquez, D.G. Stokes, Hypoxia inducible factor-1 alpha expression in human normal and osteoarthritic chondrocytes, Osteoarthritis Cartilage 12 (4) (2004) 336–345, https://doi.org/10.1016/j.joca.2003.12.005.
[13] K. Schrobback, J. Malda, R.W. Crawford, Z. Upton, D.I. Leavesley, T.J. Klein, Effects of oxygen on zonal marker expression in human articular chondrocytes, Tissue Eng. 18 (9–10) (2012) 920–933, https://doi.org/10.1089/ten.TEA.2011.0088.
[14] Y.H. Hong, C.W. Park, H.S. Kim, K.C. Won, Y.W. Kim, C.K. Lee, Effects of hypoxia/ischemia on catabolic mediators of cartilage in a human chondrocyte, SW1353. Biochem Biophys Res Commun 431 (3) (2013) 478–483, https://doi.org/10.1016/j.bbrc.2013.01.035.
[15] G.L. Semenza, HIF-1 and human disease: one highly involved factor, Genes Dev. 14 (16) (2000) 1983–1991.
[16] G.L. Semenza, Hypoxia-inducible factors in physiology and medicine, Cell 148 (3) (2012) 399–408, https://doi.org/10.1016/j.cell.2012.01.021.
[17] T.G. Smith, P.A. Robbins, P.J. Ratcliffe, The human side of hypoxia-inducible factor, Br. J. Haematol. 141 (3) (2008) 325–334, https://doi.org/10.1111/j.1365-2141.2008.07029.x.
[18] K. Yudoh, H. Nakamura, K. Masuko-Hongo, T. Kato, K. Nishioka, Catabolic stress induces expression of hypoxia-inducible factor (HIF)-1 alpha in articular chondrocytes: involvement of HIF-1 alpha in the pathogenesis of osteoarthritis, Arthritis Res. Ther. 7 (4) (2005) R904–R914, https://doi.org/10.1186/ar1765.
[19] D. Pfander, T. Cramer, B. Swoboda, Hypoxia and HIF-1alpha in osteoarthritis, Int. Orthop. 29 (1) (2005) 6–9, https://doi.org/10.1007/s00264-004-0618-2.
[20] K. Cao, Y. Pan, L. Yu, X. Shu, J. Yang, L. Sun, L. Sun, Z. Yang, Y. Ran, Monoclonal antibodies targeting non-small cell lung cancer stem-like cells by multipotent cancer stem cell monoclonal antibody library, Int. J. Oncol. 50 (2) (2017) 587–596, https://doi.org/10.3892/ijo.2016.3818.
[21] X. Shu, K.Y. Cao, H.Q. Liu, L. Yu, L.X. Sun, Z.H. Yang, C.A. Wu, Y.L. Ran, Alpha-enolase (ENO1), identified as an antigen to monoclonal antibody 12C7, promotes the self-renewal and malignant phenotype of lung cancer stem cells by AMPK/mTOR pathway, Stem Cell Res. Ther. 12 (1) (2021) 119, https://doi.org/10.1186/s13287-021-02160-9.
[22] F.H. Schopf, M.M. Biebl, J. Buchner, The HSP90 chaperone machinery, Nat. Rev. Mol. Cell Biol. 18 (6) (2017) 345–360, https://doi.org/10.1038/nrm.2017.20.
[23] B. Mi, G. Liu, W. Zhou, H. Lv, Y. Liu, J. Liu, Identification of genes and pathways in the synovia of women with osteoarthritis by bioinformatics analysis, Mol. Med. Rep. 17 (3) (2018) 4467–4473, https://doi.org/10.3892/mmr.2018.8429.
[24] Z. Fan, G. Tardif, D. Hum, N. Duval, J.P. Pelletier, J. Martel-Pelletier, Hsp90{beta} and p130(cas): novel regulatory factors of MMP-13 expression in human osteoarthritic chondrocytes, Ann. Rheum. Dis. 68 (6) (2009) 976–982, https://doi.org/10.1136/ard.2008.092288.
[25] Q.H. Ding, Y. Cheng, W.P. Chen, H.M. Zhong, X.H. Wang, Celastrol, an inhibitor of heat shock protein 90β potently suppresses the expression of matrix metalloproteinases, inducible nitric oxide synthase and cyclooxygenase-2 in primary human osteoarthritic chondrocytes, Eur. J. Pharmacol. 708 (1–3) (2013) 1–7, https://doi.org/10.1016/j.ejphar.2013.01.057.
[26] V. Calamia, M.C. de Andrés, N. Oreiro, C. Ruiz-Romero, F.J. Blanco, Hsp90β inhibition modulates nitric oxide production and nitric oxide-induced apoptosis in human chondrocytes, BMC Muscoskel. Disord. 12 (2011) 237, https://doi.org/10.1186/1471-2474-12-237.
[27] M. Siebelt, H. Jahr, H.C. Groen, M. Sandker, J.H. Waarsing, N. Kops, C. Müller, W. van Eden, M. de Jong, H. Weinans, Hsp90 inhibition protects against biomechanically induced osteoarthritis in rats, Arthritis Rheum. 65 (8) (2013) 2102–2112, https://doi.org/10.1002/art.38000.
[28] X. Kong, Z. Lin, D. Liang, D. Fath, N. Sang, J. Caro, Histone deacetylase inhibitors induce VHL and ubiquitin-independent proteasomal degradation of hypoxia-inducible factor 1alpha, Mol. Cell Biol. 26 (6) (2006) 2019–2028, https://doi.org/10.1128/MCB.26.6.2019-2028.2006.
[29] T. Lao, S. Chen, N. Sang, Two mutations impair the stability and function of ubiquitin-activating enzyme (E1), J. Cell. Physiol. 227 (4) (2012) 1561–1568.
[30] D. Liang, X. Kong, N. Sang, Effects of histone deacetylase inhibitors on HIF-1, Cell Cycle 5 (21) (2006) 2430–2435, https://doi.org/10.1002/jcp.22870.
[31] Y. Wang, C. Wu, J. Tao, D. Zhao, X. Jiang, W. Tian, Differential proteomic analysis of tibial subchondral bone from male and female Guinea pigs with spontaneous osteoarthritis, Exp. Ther. Med. 21 (6) (2021) 633, https://doi.org/10.3892/etm.2021.10065.

[32] R.S. Tuan, A.F. Chen, B.A. Klatt, Cartilage regeneration, J. Am. Acad. Orthop. Surg. 21 (5) (2013) 303–311, https://doi.org/10.5435/JAAOS-21-05-303.
[33] Q. Sun, G. Zhen, T.P. Li, Q. Guo, Y. Li, W. Su, P. Xue, X. Wang, M. Wan, Y. Guan, X. Dong, S. Li, M. Cai, X. Cao, Parathyroid hormone attenuates osteoarthritis pain by remodeling subchondral bone in mice, Elife 10 (2021) e66532, https://doi.org/10.7554/eLife.66532.
[34] L.J. Wang, N. Zeng, Z.P. Yan, J.T. Li, G.X. Ni, Post-traumatic osteoarthritis following ACL injury, Arthritis Res. Ther. 22 (1) (2020) 57, https://doi.org/10.1186/s13075-020-02156-5.
[35] E. Schipani, H.E. Ryan, S. Didrickson, T. Kobayashi, M. Knight, R.S. Johnson, Hypoxia in cartilage: HIF-1alpha is essential for chondrocyte growth arrest and survival, Genes Dev. 15 (21) (2001) 2865–2876, https://doi.org/10.1101/gad.934301.
[36] S. Stegen, K. Laperre, G. Eelen, G. Rinaldi, P. Fraisl, S. Torrekens, R. Van Looveren, S. Loopmans, G. Bultynck, S. Vinckier, F. Meersman, P.H. Maxwell, J. Rai, M. Weis, D.R. Eyre, B. Ghesquière, S.M. Fendt, P. Carmeliet, G. Carmeliet, HIF-1α metabolically controls collagen synthesis and modification in chondrocytes, Nature 565 (7740) (2019) 511–515, https://doi.org/10.1038/s41586-019-0874-3.
[37] A.T. Rufino, S.C. Rosa, F. Judas, A. Mobasheri, M.C. Lopes, A.F. Mendes, Expression and function of K(ATP) channels in normal and osteoarthritic human chondrocytes: possible role in glucose sensing, J. Cell. Biochem. 114 (8) (2013) 1879–1889, https://doi.org/10.1002/jcb.24532.
[38] M. Cucchiarini, E.F. Terwilliger, D. Kohn, H. Madry, Remodelling of human osteoarthritic cartilage by FGF-2, alone or combined with Sox9 via rAAV gene transfer, J. Cell Mol. Med. 13 (8B) (2009) 2476–2488, https://doi.org/10.1111/j.1582-4934.2008.00474.x.
[39] A. Mobasheri, M.P. Rayman, O. Gualillo, J. Sellam, P. van der Kraan, U. Fearon, The role of metabolism in the pathogenesis of osteoarthritis, Nat. Rev. Rheumatol. 13 (5) (2017) 302–311, https://doi.org/10.1038/nrrheum.2017.50.
[40] L. Li, H. Xu, L. Qu, K. Xu, X. Liu, Daidzin inhibits hepatocellular carcinoma survival by interfering with the glycolytic/gluconeogenic pathway through downregulation of TPI1, Biofactors 48 (4) (2022) 883–896, https://doi.org/10.1002/biof.1826.